Arabian Journal of Chemistry (2019) **12**, 597–609

King Saud University

Arabian Journal of Chemistry

www.ksu.edu.sa
www.sciencedirect.com

ORIGINAL ARTICLE

A completely green approach to the synthesis of dendritic silver nanostructures starting from white grape pomace as a potential nanofactory

Katya Carbone [a,*], Mariano Paliotta [a], Laura Micheli [b], Claudia Mazzuca [b], Ilaria Cacciotti [c], Francesca Nocente [d], Alessandra Ciampa [e], Maria Teresa Dell'Abate [e]

[a] *Consiglio per la ricerca in agricoltura e l'analisi dell'economia agraria, Research Centre for Olive, Citrus and Tree Fruit, Via di Fioranello 52, 00134 Rome, Italy*
[b] *Dipartimento di Scienze e Tecnologie Chimiche, Università di Roma Tor Vergata, Via della Ricerca Scientifica, 00133 Rome, Italy*
[c] *Dipartimento di Ingegneria, Università degli Studi di Roma "Niccolò Cusano", INSTM RU, Via Don Carlo Gnocchi 3, 00166 Rome, Italy*
[d] *Consiglio per la ricerca in agricoltura e l'analisi dell'economia agraria, Research Centre for Engineering and Agro-Food Processing, Via Manziana 30, 00189 Rome, Italy*
[e] *Consiglio per la ricerca in agricoltura e l'analisi dell'economia agraria, Research Centre for Agriculture and Environment, Via della Navicella 2/4, 00184 Rome, Italy*

Received 22 March 2018; accepted 1 August 2018
Available online 14 August 2018

KEYWORDS

Agro-food wastes;
Grape pomace;
Green synthesis;
Dendritic silver nanostructures

Abstract A simple, eco-friendly, cost-effective and rapid microwave-assisted method has been developed to synthetize dendritic silver nanostructures, composed of silver nanoparticles (AgNPs), using white grape pomace aqueous extract (WGPE) as both reducing and capping agent. With this aim, WGPE and $AgNO_3$ (1 mM) were mixed at different ratio, and microwave irradiated at 700 W, for 40 s. To understand the role of bioactive compounds involved in the green synthesis of AgNPs, preliminary chemical characterization, FT-IR analysis and ^1H NMR metabolite profiling of WGPE were carried out. The effects of bioactive extract concentration and stability over time on AgNPs formation were also evaluated. WGPE-mediated silver nanostructures were then characterized by UV–vis, FTIR analyses, and scanning electron microscopy. Interestingly, the formation of dendritic nanostructures, originated from the self-assembly of Ag rounded nanoparticles (average diameter of 33 ± 6 nm), was observed and ascribed to the use of microwave power and the presence of organic

* Corresponding author.
E-mail address: katya.carbone@crea.gov.it (K. Carbone).
Peer review under responsibility of King Saud University.

Production and hosting by Elsevier

https://doi.org/10.1016/j.arabjc.2018.08.001
1878-5352 © 2018 The Authors. Production and hosting by Elsevier B.V. on behalf of King Saud University.
This is an open access article under the CC BY-NC-ND license (http://creativecommons.org/licenses/by-nc-nd/4.0/).

components within the used WGPE, inducing an anisotropic crystal growth and promoting a diffusion-limited aggregation mechanism. The bio-dendritic synthetized nanostructures were also evaluated for potential applications in bio-sensing and agricultural fields. Cyclic voltammetry measurements in 0.5 M phosphate + 0.1 M KCl buffer, pH 7.4 showed that green AgNPs possess the electroactive properties typical of AgNPs produced using chemical protocol. The biological activity of synthetized AgNPs was evaluated by in-vitro antifungal activity against *F. graminearum*. Additionally, a phytotoxicity evaluation of synthetized green nanostructures was carried out on wheat seed germination. Results highlighted the potential of WGPE as green agent for bio-inspired nanomaterial synthesis, and of green Ag nanostructures, which can be used as antifungal agent and in biosensing applications.

© 2018 The Authors. Production and hosting by Elsevier B.V. on behalf of King Saud University. This is an open access article under the CC BY-NC-ND license (http://creativecommons.org/licenses/by-nc-nd/4.0/).

1. Introduction

Over the past two decades, biotechnologies have provided a boost for innovation and sustainability in many economies all around the world by developing new processes and products in a bio-economy approach. One of the most innovative and promising sectors of the bio-economy is related to the bio-based products, obtained in part or entirely from organic biomass, which account for about 16% of world production of the bio-economy's products. In the past few years, a growing number of studies on bio-inspired nanomaterials were published (Saratale et al., 2018; Vitiello et al., 2018). Among nanomaterials, metallic nanoparticles (MNPs) are the most promising ones due to their biological properties (e.g. antimicrobial, antifungal, anti-inflammatory properties). The most frequently synthetized MNPs are made of silver, gold, copper, palladium, platinum, selenium and iron, which are characterized by different biological activities. As a consequence, MNPs have possible applications in different areas from life science to high-tech sector (Carbone et al., 2016). In particular, nanostructured materials provide new and powerful tools for biomedical applications since their dimensions are close to those of biological molecules and entities (e.g. antibodies, membrane receptors, nucleic acids and proteins). Besides, nanotechnology can help the environment, for example, using nanopouros material like zeolites for soil improvement, as well as the bioremediation of wastewater. In this regard, several studies have demonstrated the effectiveness of using zeolites from oil palm ash as a low-cost adsorbent in the removal of dyes and other pollutants from wastewater (Khanday et al., 2017a; Khanday et al., 2017b).

A variety of chemical and physical procedures are available for the synthesis of MNPs, ranging from chemical reduction to laser (pulse) ablation (Ealia and Saravanakumar, 2017; Gupta et al., 2017). However, physical and chemical methods are time consuming, expensive and often involve the use of toxic solvents, with generation of hazardous by-products, low material conversions and high-energy requirements (Logeswari et al., 2013). Therefore, the synthesis of MNPs using biomimetic approaches, which are non-toxic and eco-friendly, is attractive for the realization of a more economical MNP synthetic route and when the nanostructured materials are meant for invasive applications in medicine or used in textile production (Carbone et al., 2016).

In this regard, plant mediated nanoparticle synthesis, using both whole organisms and cell free extracts, is very attractive because it is easy, less expensive than microbial alternatives, eco-friendly and safer with sustainable commercial viability. Khalil et al. (2014) also reported that plants accelerate the rate of metal ion reduction if compared to microorganisms, producing stable MNPs. Moreover, the use of plants for nanoparticles synthesis can be advantageous when compared to microbial processes, since it allows to eliminate the elaborate process of maintaining cell cultures. Besides, plant derived nanostructured materials are free of toxic contaminants, which makes them particularly suitable for therapeutic purposes (Mittal et al., 2013); the synthesis is reproducible and easy to scale-up and the green particles are highly stable (Rajan et al., 2015).

In this context, the biogenic approach to nanomaterials and MNPs synthesis using fruit and more generally plant waste (e.g. leaves) is a relatively new and largely unexplored area of nanoscience research and an innovative trend in the valorization of agricultural waste and by-products (Carbone et al., 2016; Khanday and Hameed, 2018).

Phytochemicals from plants, in addition to reducing sugars, proteins and other bioactive molecules, with antioxidant or reducing properties, are both able to reduce metal compounds into their respective nanoparticles and to stabilize them, acting as capping agents. In this regard, the valorization of by-products and/or waste of plant origin, as an inexpensive source of these compounds, is a promising sector, especially for the wine industry, where the winery by-products still contain large quantities of polyphenolic compounds and other metabolites, with high reducing power (Cecchini et al., 2013). On account of these issues, agrifood waste extracts have proved to be effective alternatives for an ecofriendly and cost-effective synthesis of NPs. Up to date, only few reports have been published on the synthesis of MNPs using fruit and vegetable peels and seeds (Rajan et al., 2015). Khadri et al. (2013) reported the synthesis of Ag nanoparticles with an average particle size of 30 nm from olive seed extract. Besides, different peel extracts from Annona squamosa, mango and Citrus sinensis fruits were reported as efficient reducing agents of Ag ions. Newly, Carbone et al. (2015) reported preliminary results that highlighted the potential of winery by-products as innovative, inexpensive, green agents for the synthesis of bio-inspired nanomaterials, with optical and electrochemical characteristics similar to ones of conventional AgNPs. To the best of our knowledge, the use of white grape pomace extract (WGPE) has not been yet investigated so far for its ability in the biosynthesis of metal nanoparticles. In light of this, the present study

aimed to assess the feasibility of using winery by-products in the preparation of silver NPs through a simple and rapid microwave-assisted method of green synthesis. The influence of different WGPE concentrations on the synthesis of AgNPs was evaluated. Obtained WGPE-mediated AgNPs were characterized by different spectral, electrochemical and morphological analyses and their stability was assessed over the time. In order to identify the biomolecules responsible for the reduction and stabilization of metal nanoparticles, for the first time, both ^{1}H NMR metabolite profiling and FTIR spectral analysis of grape pomace extract were carried out. FTIR spectroscopy was also employed to analyze the interaction of nanoparticles with the biomolecules present in WGPE. In addition, the antifungal activity of WGPE-mediated AgNPs was investigated by in vitro assay, for the first time, against *Fusarium graminearum*. Besides, the phytoxicity of biosynthesized AgNPs was also evaluated on wheat seed germination.

2. Experimental

2.1. Plant material and chemicals

White grape pomace from Malvasia di Candia cultivar was collected from local organic wineries soon after the vinification process and freeze-dried in laboratory without any pretreatment.

All reagents used in the present study were of analytical grade. Silver nitrate, silver nanoparticles dispersion (0.02 mg mL^{-1} in aqueous buffer, containing sodium citrate as stabilizer, 20 nm particle size), Folin-Ciocalteu reagent, 2,2-diphenyl-1-picrylhydrazyl radical (DPPH·), 2,2′-azinobis-(3-ethylbenzothiazolin-6-sulfonic acid) (ABTS), potassium persulfate, and vanillin were purchased from Sigma-Aldrich (Milan, Italy), while the employed water was previously purified in a Milli-Q system (Millipore, Milan, Italy) and then autoclaved.

2.2. Preparation and preliminary characterization of white grape pomace extract (WGPE)

Freeze-dried white grape pomace (1.0 g) was extracted with 10 mL of autoclaved milliQ water. The mixture was exposed to microwave heating for 40 s at 700 W and then stirred at 150 rpm, at room temperature and in the dark for 30 min. The resulting crude extract was centrifuged at 7000*g* for 15 min at 4 °C and the obtained supernatant (WGPE) was used as reducing and capping agent in the green synthesis of AgNPs. WGPE was characterized as follow: the pH value was measured using a digital pH-meter (785 DMP, Methrom, Milan, Italy), while the total titratable acidity (TA) was measured by titration of WGPE with 0.1 N sodium hydroxide (data were expressed as meq L^{-1}). Moreover, WGPE reducing capacity was assessed by Folin-Ciocalteu reagent and expressed as mg gallic acid equivalents (GAE) L^{-1} according to Carbone et al. (2011).

2.3. ^{1}H NMR metabolite profiling and FTIR spectral analysis of WPGE

In order to identify the biomolecules responsible for the reduction and stabilization of metal nanoparticles, both ^{1}H NMR metabolite profiling and Fourier Transform Infrared (FTIR) spectral analysis of WGPE were carried out as follows.

Concerning ^{1}H NMR measurements, 800 μL of WGPE were transferred in a NMR tube for the spectroscopic analysis by adding 150 μL of D_2O and 10 μL of 3-(trimethylsilyl)-propionic-2,2,3,3-d4 acid sodium salt (TSP) 10 mM solution. ^{1}H NMR spectra were recorded at 298 K with a Bruker (Milano, Italy) AVANCE spectrometer operating at a frequency of 400.13 MHz. The spectrum was acquired using 32 K data points over a 7211.54 Hz spectral width and adding 1 k transients. A recycle delay of 5 s and a 90° pulse of 14.5 μs were set up, with an acquisition time of 2.56 s. Saturation of residual water signal was achieved by irradiating it during the recycle delay at δ equal to 4.703 ppm. After the spectral integration, the concentration of some metabolites was calculated with respect to the internal standard TSP, assigned to the chemical shift 0.0 ppm.

Moreover, FTIR spectra of WGPE and WGPE- mediated AgNP samples were acquired on a Thermo-Scientific (mod. Is50) instrument (Thermo Scientific Inc., Madison WI), equipped with an attenuated total reflectance (ATR) ZnSe cell. Spectra were collected by dipping the solution directly on the entire ATR crystal and then left to dry. After that, a total of 128 scans at a resolution of 2 cm^{-1} in the 4000–700 cm^{-1} region were collected for each sample. All experiments were performed in triplicate.

2.4. Green synthesis of silver nanoparticles

Silver nanoparticles were synthesized with the assistance of microwave (MW) irradiation. The reaction conditions used for the WGPE-mediated biosynthesis of AgNPs were prior optimized (data not shown) and finally 4 mL of freshly prepared $AgNO_3$ aqueous solution (1 mM) were mixed with a known volume (0.5–2.0 mL) of WGPE and autoclaved milliQ water was added to reach a final volume of 8 mL, at pH 8.0 (by adding 0.1 N NaOH) in a 100 mL conical flask. The biosynthesis of silver NPs was carried out in a domestic microwave oven (Whirlpool MWD27, Italy) operating at 700 W and 2450 MHz for 40 s. The bio-reduction of Ag^{+} ions to AgNPs was followed by the visual observation of the color change of the solution from pale yellow to brownish-yellow and then confirmed by UV–vis spectral analysis (see below). Obtained colloidal suspensions using different WGPE concentrations were then cooled to room temperature in the dark for 1 h. Free biomolecules not absorbed onto AgNPs were then removed by repeated centrifugation at 15,000*g* for 20 min at 4 °C, followed by dispersion of the pellet in milliQ water. A calibration curve based on external standard solutions of commercial AgNPs was obtained for the quantification of biosynthesized nanoparticles. Suitable controls were maintained throughout the trials.

2.5. UV–vis and morphological characterizations of WGPE-mediated AgNPs

Preliminary characterization of WGPE-mediated silver nanoparticles was carried out using UV–vis spectroscopy (Evolution 300, THERMO Scientific, Italy). The bio-reduction of Ag^{+} ions in solution was monitored in the wavelength range of 250–600 nm, at a resolution of 1.5 nm (scan

speed: 120 nm min^{-1}; data interval: 0.2 nm), and using autoclaved milliQ water as the blank.

The morphology of WGPE-mediated AgNPs was investigated by means of field-emission gun scanning electron microscopy (FEG-SEM) (Cambridge Leo Supra 35, Carl Zeiss), after sputter-coating with gold under argon atmosphere (25 mA, 120 s). Energy Dispersive Spectroscopy (EDS) microanalysis of Ag element was performed by means of INCA Energy 300, Oxford ELXII detector. The average particles diameter was determined considering randomly selected particles from SEM micrographs (ImageJ, NIH). As a reference, commercial AgNPs were also observed at SEM.

2.6. Electrochemical characterization of WGPE- mediated AgNPs

All electrochemical measurements were performed by means of a computer controlled system (AUTOLAB, model PGSTAT 12) equipped with GPES software (ECO-CHEMIE, the Netherlands). Screen Printed Electrodes (SPEs) were prepared in the Laboratory of Analytical Chemistry of the University of Rome "Tor Vergata". SPEs were printed with a 245 DEK (Weymouth, UK) screen-printing machine. The ink used to print the working and counter electrodes was a graphite-based ink (Electrodag 423 SS from Acheson Milan, Italy), while the ink used to print the reference electrode was a silver one (Electrodag 477 SS, from Acheson Milan, Italy). A flexible polyester film (Autostat HT5, Autotype Italia, Milan, Italy) was used as a support. The diameter of the working electrode was 0.3 cm and its geometric area was 0.07 cm^2.

Samples of WGPE-mediated silver nanoparticles were characterized by cyclic voltammetry (CV) by direct detection of nanoparticles. Moreover, the matrix (WGPE before the addition of $AgNO_3$) was analyzed by CV in order to observe the possible presence of electroactive compounds that could interfere with the analysis of nanoparticles.

The CV measurements were carried out in "drop" (60 μL), diluting the sample 1:1 v/v in 0.5 M phosphate buffer + 0.1 M KCl, pH 7.4. Reported data were obtained from three independent experiments with three replicates.

2.7. In vitro antifungal activity and seed toxicity of WGPE-mediated AgNPs

The antifungal activity of WGPE-mediated silver nanoparticles was evaluated by considering the inhibitory effect on the mycelial growth of *Fusarium graminearum*, the causal agent of the *Fusarium* Head Blight (FHB). Potato Dextrose Agar (PDA; Formedium, Hunstanton, England) plates (60 mm) were prepared by adding 1 mL of four different concentrations (23.8, 36.4, 73.9 and 98.8 μg mL^{-1}, respectively) of green AgNPs to 9 mL of PDA. Media plates amended with commercial AgNPs (Sigma-Aldrich, Italy) or WGPE were also prepared.

For the bioassay, 4-mm diameter mycelia disc from 7 day-old culture was placed in the center of the PDA plates, prepared as described above. The plates were incubated at 22 °C in the dark. After four days from inoculation, the colony diameters were measured and the percentage growth inhibition was calculated in reference to the growth of the colony on PDA. Two replications were prepared for each treatment and each experiment was replicated twice.

A seed toxicity assay was also performed to test the effect of WGPE-mediated silver nanoparticles on wheat seed germination.

For this purpose, seeds of the durum wheat (*T. turgidum* ssp. *durum*) cultivar "Core" were treated with the four AgNPs doses described before. Briefly, 50 seeds were immersed in a 1% sodium hypochlorite solution for 10 min to ensure surface sterility and then were washed three times with sterile water. The treatment was performed by soaking the seeds with 3 mL of the four AgNP solutions for 1 h, at 20 °C, by 200 rpm constant shaking. Treated seeds were immediately transferred onto Petri dishes containing sterile water soaked filter paper and were incubated in a growth chamber at 20 °C. Two replications for each dose of WGPE-AgNPs were applied. Seed germination was monitored daily until 6 days after treatments, and compared to the untreated material.

2.8. Statistical analysis

Described analyses were carried out in triplicate. Statistical analysis of data expressed as mean ± standard deviation, and mean testing (Duncan's range test) with level of significance set at $p \leq 0.05$ were performed with the SPSS 17.0 software (SPSS, Inc., Chicago, Illinois), unless differently specified.

3. Results and discussion

3.1. Characterization and chemical profiling of white grape pomace extract (WGPE)

The so-called "wine grape pomace", which is the main winery by-product, is a valuable source of polyphenols, especially the one from white grape varieties (Cecchini et al., 2013). Table 1 shows the main chemical parameters of WGPE used in the present study.

Literature data highlighted the role of polyphenols in plant extracts as reducing/capping agent in the green synthesis of metallic nanoparticles (Mittal et al., 2013). However, there is a lack of information about the total phenolic content (TPC) of plant extracts used for this purpose. This is a very important information regarding the standardization of the AgNPs synthesis protocol, as TPC is generally used to measure the average reducing power of plant extracts (Huang et al., 2005). In this regard, we found only one publication reporting the average TPC of plant extract used in the biosynthesis of silver

Table 1 Physical-chemical characteristics of WGPE (mean ± s.d.).

Parameter	Value
pH	3.18 ± 0.02
TA (meq L^{-1})[a]	67 ± 1
TPC (mg/L)[b]	294 ± 9

[a] TA: titratable acidity.
[b] TPC: total phenolic content (expressed in terms of mg gallic acid equivalents (GAE) L^{-1}).

nanoparticles (Makris et al., 2007). In the present study, a WGPE with an initial standardized TPC of 294 mg/L was used in all synthesis experiments (Table 1).

To better understand the role of different plant metabolites involved in the biosynthesis of silver nanoparticles, a FTIR spectral analysis of WGPE was carried out.

As shown in Fig. 1, in the spectrum of WGPE (spectrum A) several diagnostic bands are present: the broad band at 3300 cm^{-1} is due to the stretching of the O—H groups, while the two peaks at 3310 and 3250 cm^{-1} account for the stretching of N—H present in the amino or amide groups. Bands in the 3000–2800 cm^{-1} and 1400–1300 cm^{-1} regions are associated to C—H stretching and bending, respectively. Furthermore, the bands in the 1900–1450 cm^{-1} region are due to the stretching of the C═O group present in different environments (i.e., acid, ester and keto groups, in unconjugated and conjugated molecules, amide groups) as well as C═C stretch in aromatics. Finally, the bands at about 1260 cm^{-1} and 1040 cm^{-1} are due to the stretching of C—O in esters and alcohol, respectively.

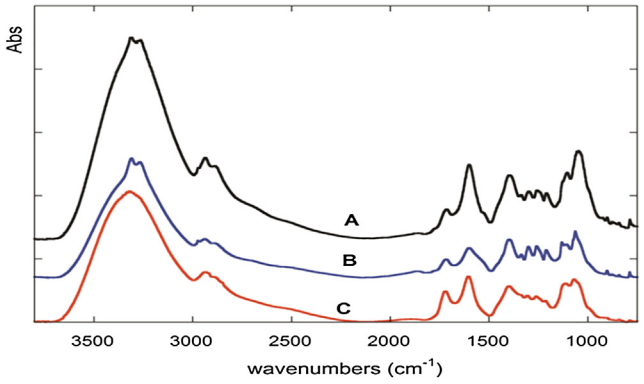

Fig. 1 FTIR spectra of (A): WGPE alone; (B): WGPE-mediated NPs obtained by adding 1.5 mL of WGPE in $AgNO_3$ solution; (C): WGPE-mediated NPs obtained by adding 1.0 mL of WGPE in $AgNO_3$ solution.

These results are compatible with the presence, in WGPE, of molecules like polysaccharides, proteins, terpenoids, and flavonoids (Song et al., 2009). To better identify the biomolecules acting as reducing and capping agents, ^{1}H NMR based metabolite profiling of WGPE was also carried out. NMR spectroscopy can analyze many compounds simultaneously and provide a well-defined molecular profile in few minutes, requiring very small volumes of sample.

In Fig. 2, three main WGPE ^{1}H NMR spectral regions were identified as follow: (1) aromatic region (> 5.5 ppm), (2) carbohydrate region (between 5.5 and 3.0 ppm), and (3) organic and amino acid region (< 3.0 ppm).

The metabolite assignment was achieved using literature data (Gallo et al., 2014; López–Rituerto et al., 2012; Picone et al., 2011). In the present study, 25 metabolites were unequivocally assigned (Table 2). Several phenolic compounds, as gallic acid, trans-caffeic acid, resveratrol, caftaric acid and epicatechin, were identified in the aromatic region (Gallo et al., 2014; López–Rituerto et al., 2012; Picone et al., 2011; Anastasiadi et al., 2009).

These secondary metabolites act as reducing and stabilizing agents for the bioreduction of the synthesized novel metallic nanoparticles (Kuppusamy et al., 2016). They are different

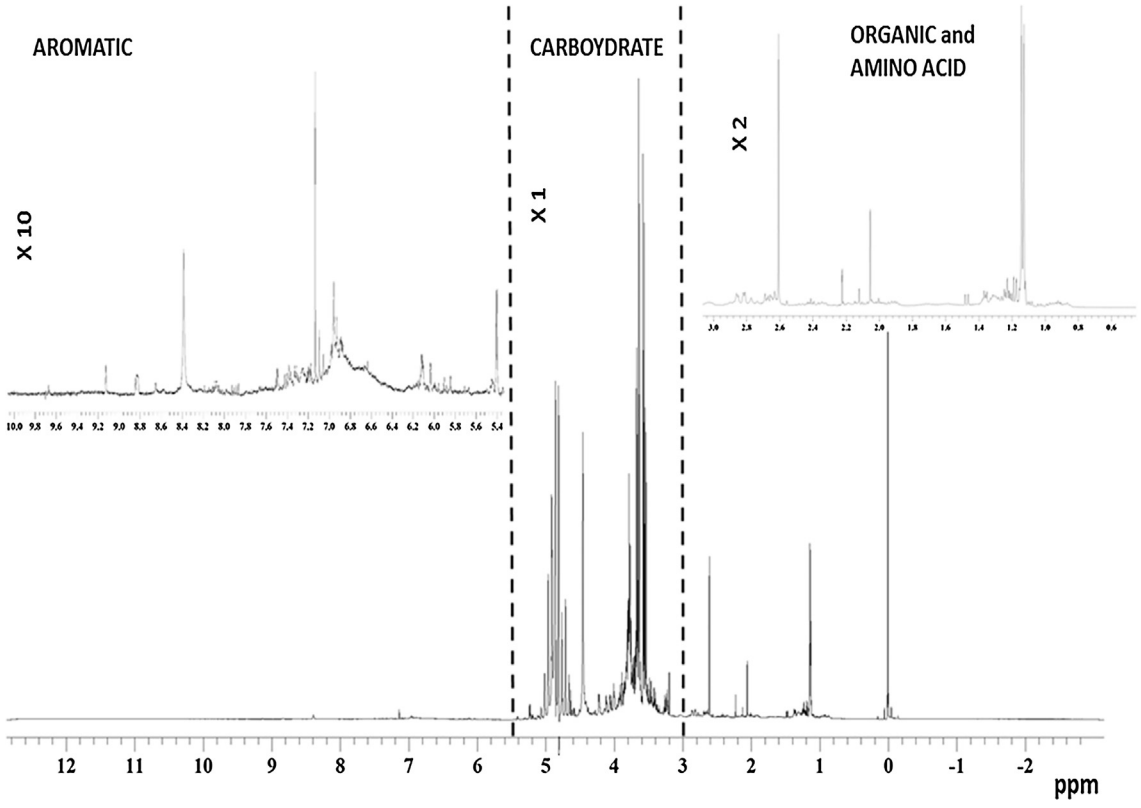

Fig. 2 400.13 MHz ^{1}H NMR spectrum of white grape pomace aqueous extract (WGPE).

Table 2 ^{1}H NMR Chemical shifts (ppm) of the 25 metabolites detected in WGPE.

Compound	ppm	Multiplicity* and assigment
1-Propanol	0.88	t (CH_3)
Leucine	0.95	d, (CH_3)
2,3-Butanediol	1.13	d, (CH_3)
Alanine	1.48	d, (CH_3)
Acetic acid	2.05	s, (CH_3)
Valine	2.31–2.35, 1.05, 0.99	m (CH), d (CH_3), d (CH_3)
Succinic acid	2.61	s (CH_2)
Malic acid	2.85	dd (CH_2)
Choline	3.19	s (CH_3)
Glicerol	3.53–3.67	dd, dd (CH_2)
Tartaric acid	4.45	s (CH)
Glucose	5.23. 4.64	d (CH_2), d (CH_2)
Ribose	5.39, 5.25, 4.93, 4.07–4.16	d (CH_2), d (CH_2), d (CH_2), m (CH)
Mannnose	5.18, 3.92–3.96	d (CH_2), m (CH)
Galactose	5.25, 5.22. 3.98, 3.93	d (CH_2), d (CH_2), d (CH_2), d (CH_2)
Arabinose	5.30, 5.24, 4.52	d (CH_2), d (CH_2), d (CH_2),
Epicatechin	6.97, 6.79, 6.77, 5.94, 5.92, 4.81, 4.18, 2.85, 2.74	d (CH), m (CH), m (CH), d (CH), d (CH), s (CH), m (CH), dd (CH_2), dd (CH_2)
Gallic acid	7.13	s (CH)
Caftaric acid	7.18, 7.09, 6.89, 5.42, 4.74	d (CH), d (CH), d (CH), dd (CH), d (CH)
trans-Caffeic acid	7.50, 7.09, 6.93, 6.80	d (CH), d (CH), dd (CH), d (CH)
Resveratrol	7.39, 7.05, 6.88–6.91	d (CH), d (CH), m (CH)
Formic acid	8.39	S (HCO_2H)
Histidine	8.66, 7.39	s (CH), s (CH)
Trigonelline	9.12, 8.82, 8.01	m (CH), m (CH), s (CH)
Ethanal	9.66s	s (CHO)

* Abbreviations: s = singlet; d = doublet; m = complex multiplet; t = triplet.

types of antioxidants (Fig. 3) that reduce the metal ions by their functional groups (Malešev and Kuntić, 2007; Makarov et al., 2014) in the ionic or electrostatic interactions with the metal complexes.

The mechanisms of action in the complexing activity of these compounds take into consideration the hydroxyl groups: their deprotonation yields to anionic stabilized species by resonance phenomena; their stability is enhanced by the presence of a H bonding pattern (Leopoldini et al., 2011). For example, gallic acid, caffeic acid, epicatechin are excellent free radical scavengers by H atom donation (Leopoldini et al., 2011).

The presence of all these compounds in a unique natural extract, WGPE, consistently increases the antioxidant activity of the final product with respect to each single metabolite. There are not, at our best knowledge, NMR data on these model systems, which should be further investigated. In addition, using NMR spectroscopy it should be possible to study the extent of the interaction of each secondary identified metabolite (Table 2 and Fig. 3), through their quantification, in the mechanisms of antioxidant systems: from these data it will be possible, in further studies, to obtain also new information on the involved kinetic processes. In the present study, the following concentrations in the aqueous WGPE were quantified: 4.1×10^{-5} and 1.9×10^{-5} mol L^{-1} respectively for epicatechin and gallic acid; 7.6×10^{-6} mol L^{-1} for caffeic and caftaric acids, and finally for resveratrol a concentration of 4.8×10^{-6} mol L^{-1} was found.

3.2. Spectral studies on WGPE-mediated AgNPs

Bio-reduction of Ag^{+} ions in solution was monitored by visual observation and confirmed by using UV–vis spectral analysis. Due to the addition of WGPE, 1 mM solution of $AgNO_3$ changed from colorless to yellowish brown in the experimental condition adopted (inset, Fig. 4), due to the excitation of surface plasmon resonance (SPR) vibration of NPs. The characteristic SPR peak was observed at 431.6 nm (Fig. 4). Compared to a commercial standard suspension of AgNPs (20 nm sized), SPR peak of WGPE-mediated AgNPs shifted

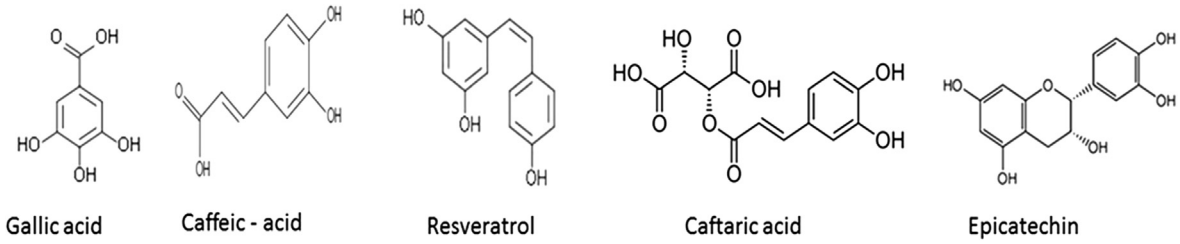

Fig. 3 Structures of the phenolic compounds identified in WGPE using ^{1}H NMR.

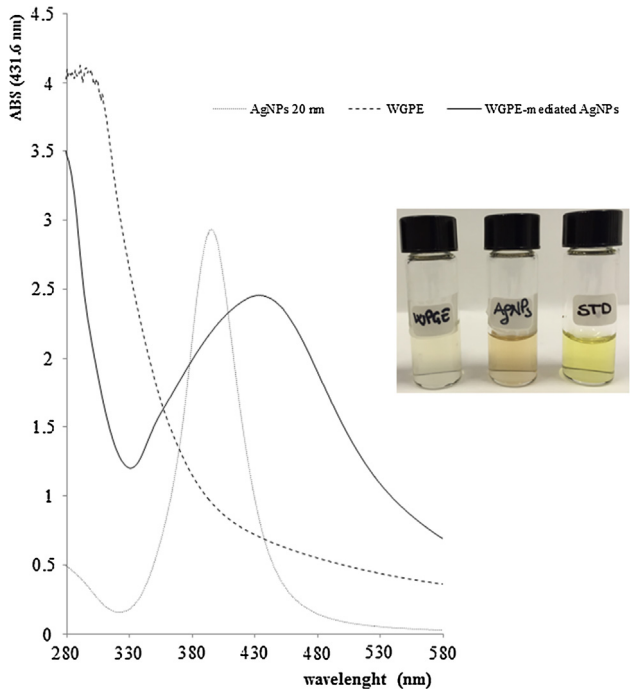

Fig. 4 Visual observations (inset) and UV–vis absorption spectra of WGPE, WGPE-mediated AgNPs, and standard AgNPs (20 nm).

to the red (from 394.6 to 431.6 nm), with a simultaneous broadening of the band, indicating an increase in the particle size (Bar et al., 2009). However, the SPR peak of WGPE-mediated AgNPs was below 450–470 nm, which was the classical SPR wavelength range of plant-mediated synthesis of silver nanoparticles, as reported in literature (MubarakAli et al., 2011; Gnanajobitha et al., 2013). Fig. 4 also shows another peak in the UV region (280–330 nm), which is a characteristic of polyphenol compounds (Terenteva et al., 2015). As shown in Fig. 4, the intensity of this peak declined when WGPE-mediated synthesis of AgNPs took place, indicating that polyphenols acted as reducing and capping agent, as previously described (Huang et al., 2014; Terenteva et al., 2015). The ratio $AgNO_3$/WGPE (v/v) strongly affected the yield of AgNPs. It is seen from the diagram in Fig. 5 that the yield of AgNPs increased almost linearly by varying the amount of WGPE added to the silver solution from 0.5 to 2.0 mL, corresponding to a final AgNPs concentration ranging from 23.8 to 98.8 μg mL^{-1}. As a consequence, when a larger volume of WGPE (2 mL) is added to a known volume of silver nitrate solution (4 mL; 1 mM), the SPR peak centred at 431.6 nm increases in intensity, pointing out an increase in the number of metallic nanoparticles formed in the reaction medium (data not shown) (Cruz et al., 2010).

In the present study, the best results for AgNPs synthesis were obtained by using $AgNO_3$ aqueous solutions at pH 8.0, as nanoparticles formed at this pH value were more stable with no SPR peak broadening (data not shown). Khalil et al. (2014) highlighted that in the reaction the pH influences the electrical charges of biomolecules (i.e. ionization state) in the plant extract used for the green synthesis of AgNPs, affecting their capping and stabilizing abilities. In the present work, AgNPs synthesis was faster at pH 8.0, probably due to the ionization of polyphenolic compounds and other bioactive molecules (i.e. proteins) in WGPE, possessing hydroxyl and carboxyl groups, which are able to bind to metals.

Fig. 6 shows the influence of the reaction time on the intensity of SPR band of WGPE-mediated AgNPs. Data pointed out that the reduction of silver ions and optimal formation of stable AgNPs occurred within 3 h under laboratory conditions, with no significant differences between 3 and 24 h. Therefore, all further studies were carried out for 3 h. FTIR measurements were also carried out on synthetized AgNPs to identify the biomolecules present in WGPE putatively involved in the reduction and capping of green nanostructures (Fig. 1).

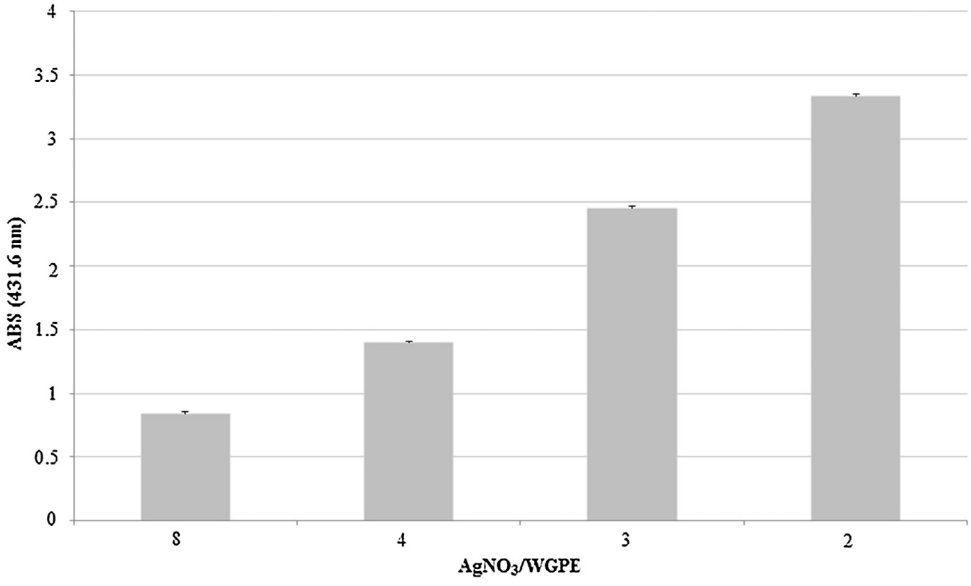

Fig. 5 Dependence of AgNPs yield on the $AgNO_3$/WGPE ratio.

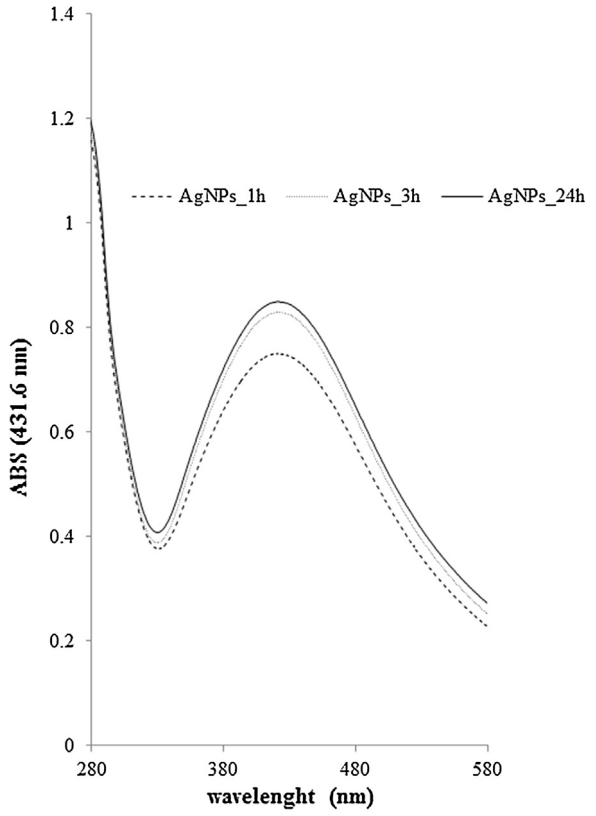

Fig. 6 Dependence of SPR band intensity of WGPE-mediated AgNPs yield on the reaction time.

The differences between spectra before (WGPE alone; spectrum A) and after NPs formation (B and C spectra) are mainly in the band envelops at 1040 cm^{-1} and 1600–1400 cm^{-1} (Fig. 1). This finding suggests that Ag^+ reduction and the subsequent coordination of WGPE compounds on the surface of the nanoparticles involve the CO, OH and NH groups present in polysaccharides, proteins, terpenoids and flavonoids (Logaranjan et al., 2012; Gan et al., 2012).

3.3. Scanning electron microscopy (SEM) and EDX analysis

It is well known that the intrinsic properties of nanoparticles strongly depend on their structure. In this regard, the morphology of the produced silver based structures was analysed by observation at SEM (Fig. 7) and the presence of Ag was confirmed by EDS microanalysis (Fig. 7c, inset).

The reported SEM micrographs show the formation of dendritic structures of different dimensions, surrounded by randomly distributed single Ag rounded nanoparticles with an average diameter of 33 ± 6 nm (Fig. 7c–f), higher with respect to the commercial standard AgNPs (average diameter of 18 ± 3 nm, Fig. 7a and b). The higher average diameter of the obtained WGPE-derived AgNPs can be ascribed to the presence of a coating based on residual WGPE components that tend to adsorb on the particles surface due to their very high specific surface area, as evident in Fig. 7f and pointed out by FTIR analysis.

Moreover, the obtained dendritic silver structures were characterized by well-defined trunk and branches on both sides of the trunk, composed of nanometric silver particles. The branches length ranged between 15 μm and 30 μm for the smaller structures and between 55 μm and 80 μm for the bigger ones, whereas the trunks were characterised by a length between 70 and 275 μm. It is evident that the dendritic fractal structures were hierarchically formed by the self-assembly of silver nanoparticles as basic building blocks.

In order to explain the underneath crystal growth mechanism and the resulting shape of the silver crystals, several mechanisms have been proposed in literature for the development of dendritic silver nanostructures in non-equilibrium conditions (Mandke et al., 2012; Duan et al., 2014) and, up to date, the underneath process has not been completely understood yet. Most of the proposed mechanisms are based on a diffusion limited aggregate (DLA) model, according to which the dendritic structure is formed from the asymmetric growth of silver nanoparticles when the growth rate is limited by the rate of diffusion of solute atoms to the interface. A layer-by-layer mechanism has been proposed: AgNPs tend to locally aggregate forming Ag nanoparticle layers and on a compact layer AgNPs can aggregate and self-assemble into small dendritic structures.

In details, in the presence of reducing agents, Ag^+ ions convert to AgNPs, and, at the initial stage, silver nanoparticles grow along the [1 1 1] direction to form a trunk, being the growth promoted along the [1 1 1] direction. Then, the additional formed silver nanoparticles tend to attach to a silver trunk and their growth also begins along the [1 1 1] direction to form further secondary and tertiary branches. As the reaction proceeds with time, all the trunks, branches and leaves grow and finally interconnect to each other, leading to the formation of a dendritic structure (Wen et al., 2006; Mandke et al., 2012).

It has been demonstrated that a strong anisotropic growth contributes to the evolution of Ag nanostructure into a thermodynamic stable dendritic structure and that AgNP dendritic structures are formed at the interface when Ag ions are reduced in the presence of surfactants.

Several authors highlighted that the formation of silver hierarchical dendritic structure strictly depends on the reduction process (Alam et al., 2014), the reaction time (Lin and Kim, 2010), the concentration of the AgNP precursor (Baruwati et al., 2009), and the strength of the reducing agent (Alam et al., 2014).

In details, long reaction times lead to the obtainment of thick and brittle dendritic structures (He et al., 2010), becoming the obtained side branches of the dendritic structures less well defined, since more silver nanoparticles tend to aggregate each other into the spaces between the side branches as the reaction went on; higher AgNP precursor concentration leads to large dendritic nanostructures. According to Alam et al. (2014), a strong reducing agent (e.g. $NaBH_4$) is not able to induce the dendritic nanostructure formation and fast reduction processes lead to silver nanoparticles formation instead of dendritic structure, even if the main reason has not been well understood yet.

Furthermore, the obtained structures depend on the used process and reducing agent. For example, several authors obtained dendritic structures, using PVP as stabilizing and reducing agent by means of sonoelectrochemistry and microwave irradiation processes, demonstrating that PVP leads to the formation of side branches and leaves and promotes the

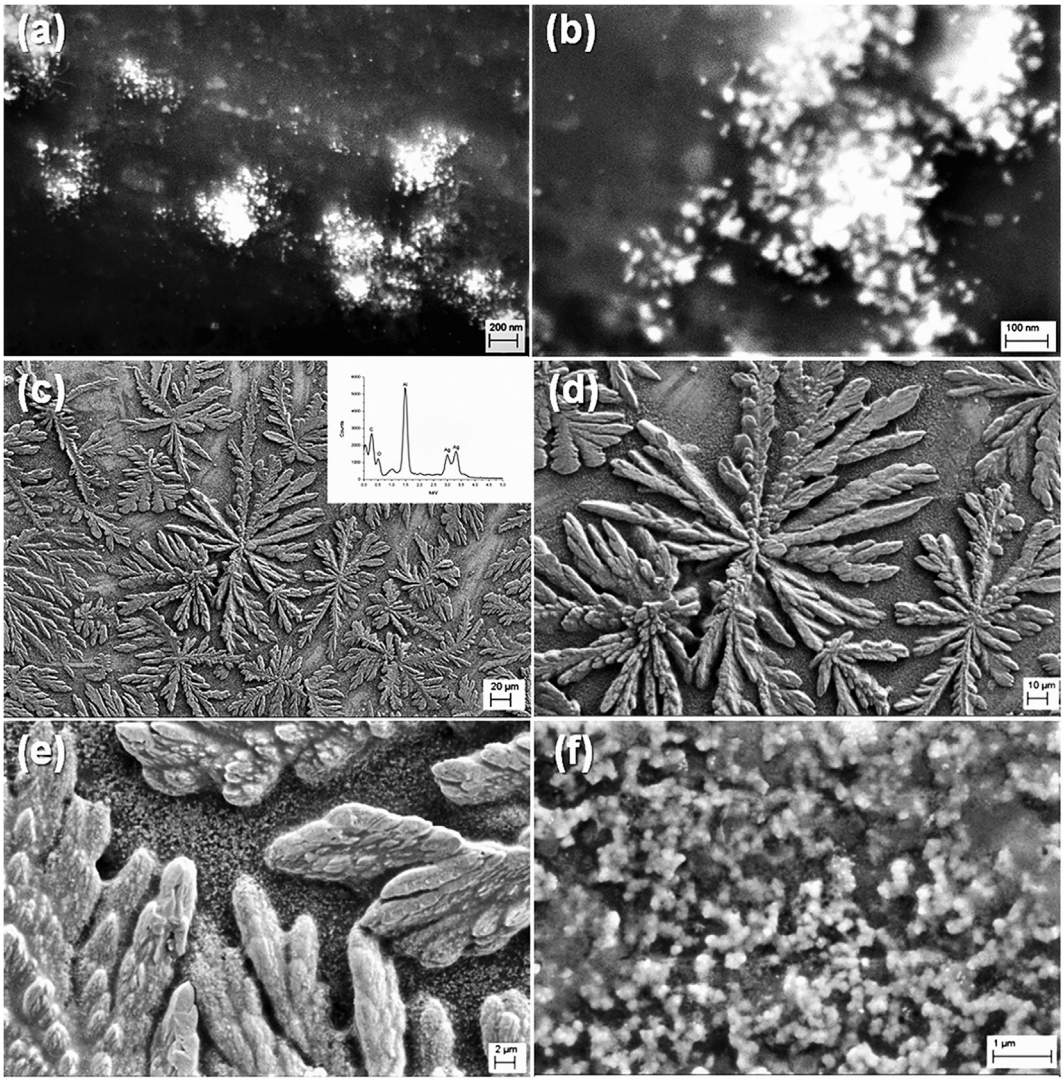

Fig. 7 SEM micrographs of the purchased AgNPs (a and b) and of the obtained WGPE-Ag NPs (c–f) (EDS spectrum for WGPE-Ag NPs, inset of (c).

formation of finer, more hierarchical microstructures (Agrawal et al., 2008; Tang et al., 2009).

Alam et al. (2014) reported that it was possible to obtain dendritic structures using disodium citrate sesquihydrate ($C_6H_6Na_2O_7{\cdot}3/2H_2O$) as reducing agent, whereas using sodium tetra hydroborate ($NaBH_4$) Ag nanoparticles are formed instead of dendritic structures (Alam et al., 2014).

Basing on these previous reports and of our results, it is possible to conclude that MW power and the presence of organic components within the used WGPE play pivotal roles in the formation of Ag dendrites.

3.4. Potential applications of WGPE-AgNPs

A preliminary evaluation on the potential applications of synthetized green nanostructures in biosensing and agriculture was carried out. At this regard, WGPE-AgNPs were investigated on the basis of their electrochemical and antifungal properties and results are discussed below.

3.4.1. Electrochemical characterization of WGPE-mediated AgNPs

Among different silver nanostructures (e.g. nanospheres, nanorods, nanosheets, and nanowires), the dendritic ones attracted considerable attention due to their high electrical conductivity and the high specific surface area that make them particularly suitable for application in the field of optoelectronics and sensors. In this regard, to evaluate the potential application of green denditric structures in sensoring field, the electrochemical properties of biosynthesized silver nanostructures were examined using cyclic voltammetry (CV). Results showed that the WGPE-AgNPs exhibit similar redox properties as solution-synthesized silver nanoparticles by modifying the Brust method or other reported in literature (Welch and Compton, 2006; Giovanni and Pumera, 2012).

Fig. 8 shows typical voltammograms of cyclic scan originating from −0.8 to +0.05 V, for blank (only buffer) and WGPE-nanostructures in solution at three different concentrations (23.8, 36.4, and 73.9 $\mu g\,mL^{-1}$). The CV of blank matrix

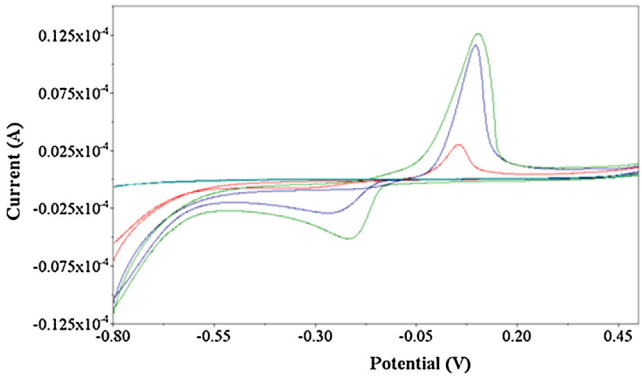

Fig. 8 Cyclic voltammetry of WGPE-mediated AgNPs (blank matrix: cyan line; AgNPs at 23.8 μg mL^{-1}: green line; AgNPs at 36.4 μg mL^{-1}: blue line; AgNPs at 73.9 μg mL^{-1}: red line).

(WGPE diluted 1:1 (v/v) in 50 mM phosphate buffer, pH 7.4) did not show any peak, index of absence of electroactive compounds in the analyzed extract.

The different dilutions of WGPE-AgNPs showed the characteristic CV profile of traditional AgNPs. There is an apparent feature of electrochemical dissolution (stripping) of silver nanostructures on the electrode surface, at ~−200 mV, and reduction of the generated silver ions in the oxidative part of cycle from the solution at ~+100 mV. As it can be seen from the voltammograms, the behavior of WGPE-mediated nanoparticles significantly differs, depending on the concentration of the nanoparticles, with a broadening of the peak at high concentrations, indicating a probable aggregation.

Giovanni and Pumera (2012) established that the electrochemical behavior of various silver nanoparticles significantly differs, depending on the size of the nanoparticles. WGPE-AgNPs showed a voltammetric profile, for potential peak values and for shape of both peaks, similar to the traditional AgNPs with size higher than 40 nm (Giovanni and Pumera, 2012), probably due the presence of organic components within the used WGPE coating agent.

Fig. 9 shows typical voltammograms after ten consecutive cyclic scans for WGPE-AgNPs. As it can be seen from the voltammograms, the potential of oxidation peak decreased upon increasing the number of scans. This reflects the fact that,

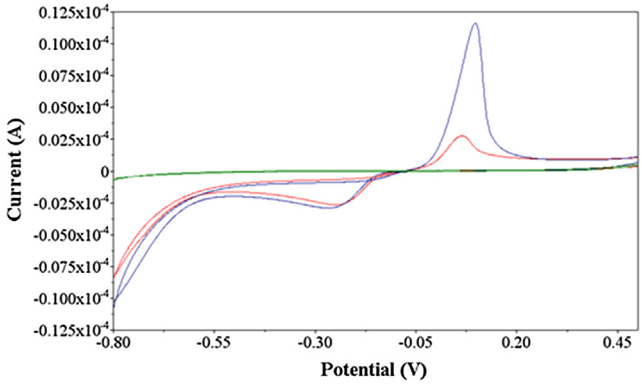

Fig. 9 Overlay cyclic voltammetry of WGPE-mediated AgNPs (one cycle: red line; after 10 cycles: black line).

during consequent reduction steps, lower and lower amount of Ag^{+} ions is available and smaller and smaller AgNPs are redeposited and consequently re-oxidized, which is a characteristic behavior of Ag-NPs (Ivanova and Zamborini, 2010).

The interaction between metal nanoparticles (MNPs) and biomolecules has led to new intriguing approaches for the immunoassays, using the electrochemical detection to obtain a high sensitivity (Welch and Compton, 2006). In this regard, the electroactive properties of WGPE-mediated AgNPs suggest the possibility to use them as an enzymeless electrochemical biosensor through the functionalization of AgNPs with a bioreceptor to recognize specific analytes. In this case, AgNPs should be the support of the bioreceptor and, at the same time, the transducer in order to detect the specific analyte (AgNPs) possess the dual role of electrochemical markers in electrochemical measurements and backing material for the bioreceptor immobilization (El-Ansary and Faddah, 2010; Nidzworski et al., 2014).

3.4.2. Antifungal activity of WGPE-mediated AgNPs

The intensive use of chemical pesticides during the last decades caused serious human and environmental hazard. Consequently, the interest towards the discovery of green formulations as alternative to the conventional plant protection products is increasing. In this contest, silver nanoparticles of either simple nature or combined with natural compounds could represent an innovative approach to plant disease control. The in-vitro antibacterial and antifungal activity of silver nanoparticles also obtained from plant extract has been demonstrated against various bacteria and fungi (Li et al., 2005; Kim et al., 2007; Jo et al., 2009; Kim et al., 2012; Thombre et al., 2012). To the best of our knowledge, this is the first time that the antifungal activity of different concentrations of WGPE-mediated AgNPs is tested against *F. graminearum*, the most important causal agent of the Fusarium Head Blight (FHB) in wheat and barley. *F. graminearum* has major economic impacts in the agriculture industry and production losses worldwide have been estimated to be as much as 50%. To evaluate the potential fungistatic activity of dendritic nanostructures, the radial growth of fungal mycelium was measured after 4 days (Fig. 10) and the growth inhibition percentage was calculated. Moreover, the antifungal activity of green Ag nanostructures against *F. graminearum* was investigated in comparison to that of a commercial suspension of standard AgNPs (20 nm) and WGPE. Results pointed out that *F. graminearum* isolate was mild sensitive to the green nanostructures and no reduction of the growth was achieved in a dose-response manner. Specifically, about 20%, 24%, and 19% of growth inhibition was recorded using 36.4, 73.9, and 98.8 μg mL^{-1} of WPGE-mediated AgNPs, respectively; whereas the lowest level of inhibition (16%) was obtained on PDA treated with 23.8 μg mL^{-1} of nanoparticles (Fig. 10). In contrast, commercial standard AgNPs, $AgNO_3$ solution (1 mM), and raw WPGE did not exert any growth inhibition activity. These preliminary findings highlight the potential of synthetized green nanostructures as a promising eco-friendly alternative to the use of chemicals for controlling plant fungal pathogens. Further research should be conducted to clarify the antifungal action mechanism of these novel green structures also taking into consideration different fungal species and strains.

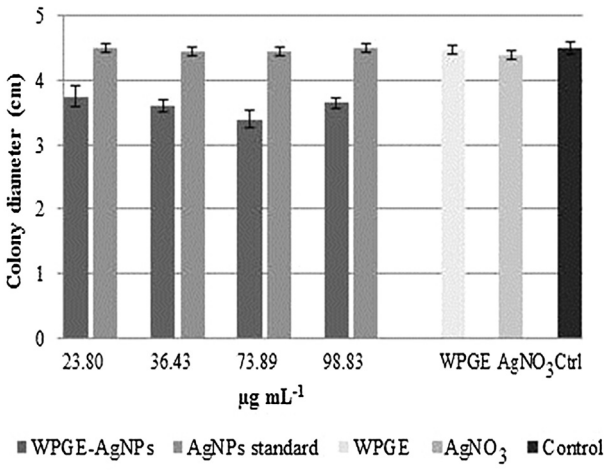

Fig. 10 Effect of WGPE-mediated AgNPs, AgNPs standard, $AgNO_3$ and WGPE on mycelia growth of Fusarium graminearum. Colony diameter (cm) 4 days post inoculation. Controls are media plate without additions.

To the best of our knowledge, in fact, there are no literature data about the antifungal activity of green silver dendrimers with which compare our results. To explain our results we can speculate that dendrimers possess an architecture that allows the organization of metal nanoparticles on their surface and/or in their interior. As a consequence, the accessibility of Ag becomes a limiting factor for a successful fungistatic action of synthetized nanostructures. Besides, an unsuitable dispersion in water of WGPE-mediated nanostructures could be responsible of the observed results as a function of different WGPE-AgNP concentration used.

To be applicable in open field, however, the assessment of a possible phytotoxic effect of WGPE-AgNPs is necessary. In this regard, and considering the limited studies on the phytotoxicity of nanoparticles (Lin and Xing, 2007), the effect of synthetized green nanostructures on durum wheat seed germination was also investigated. After 6 days of incubation, 95% of the treated seeds had germinated and developed roots and shoot. No differences of germination rate were observed with respect to control seeds treated with water, indicating that wheat seed germination was not affected by the treatment with the nanostructures, even applied at high concentrations (Fig. 11). In this study, the lack of toxicity of AgNPs on wheat seed germination, also at the highest concentration exposure, indicates a potential use of these silver nanostructures in crop plant protection.

4. Conclusion

For the first time, in the present study, an innovative green approach to the winery waste management for the synthesis of well-defined dendritic silver nanostructures, using a white grape pomace aqueous extract (WGPE) as both reducing and capping agent with the assistance of microwaves is presented. It is found that the plant extract composition and microwaves play important roles in the formation of these green dendritic structures, which can be applied both in agriculture and biosensing sectors.

Results reported herein give new insights into the valorization of agro-food waste and by-products, which are now more than ever a valuable asset in a bio-economy approach to the management of agro-industrial pipeline. Moreover, the proposed process provides the first example of the use of white grape pomace as a tool for the fabrication of nanoscale materials and also suggests a way to prepare a similar structure for

Fig. 11 Durum wheat seed germination after 6 days of incubation. A) AgNPs at 23.8 µg mL^{-1}; B) AgNPs at 36.4 µg mL^{-1}; C) AgNPs at 73.9 µg mL^{-1}; D) AgNPs at 98.8 µg mL^{-1}; E) control seeds treated with distilled water.

other noble metals, completely fulfilling the requirements of facile synthesis and green chemistry concept (i.e. aqueous medium, easy processing, surfactant or template free, low temperature, reproducibility), in comparison to the commonly used processes for the synthesis of dendritic structures.

Conflicts of interest

There are no conflicts to declare.

Acknowledgements

The authors are thankful to Dr. R. Ciccoritti for the graphical support during manuscript's preparation.

References

Agrawal, V.V., Kulkarni, G.U., Rao, C.N.R., 2008. Surfactant-promoted formation of fractal and dendritic nanostructures of gold and silver at the organic–aqueous interface. J. Colloid Interface Sci. 318, 501–506.

Alam, M.M., Ji, W., Luitel, H.N., Ozaki, Y., Watari, T., Nakashima, K., 2014. Template free synthesis of dendritic silver nanostructures and their application in surface-enhanced Raman scattering. RSC Adv. 4, 52686–52689.

Anastasiadi, M., Zira, A., Magiatis, P., Haroutounian, S.A., Skaltsounis, A.L., Mikros, E., 2009. 1H NMR-based metabonomics for the classification of Greek wines according to variety, region, and vintage. Comparison with HPLC data. J. Agr. Food Chem. 57, 11067–11074.

Bar, H., Bhui, D.K., Sahoo, G.P., Sarkar, P., Pyne, S., Misra, A., 2009. Green synthesis of silver nanoparticles using seed extract of Jatropha curcas. Colloids Surf. Physicochem. Eng. Aspects 348, 212–216.

Baruwati, B., Polshettiwar, V., Varma, R.S., 2009. Glutathione promoted expeditious green synthesis of silver nanoparticles in water using microwaves. Green Chem. 11, 926–930.

Carbone, K., Giannini, B., Picchi, V., Scalzo, R.L., Cecchini, F., 2011. Phenolic composition and free radical scavenging activity of different apple varieties in relation to the cultivar, tissue type and storage. Food Chem. 127, 493–500.

Carbone, K., Paliotta, M., Cacciotti, I., Micheli, L., 2015. Microwave-assisted green synthesis of stable silver-conjugated flavonoid nanoparticles. In: Cubbadda, F. (Ed.), Nanotechnologies and Nanomaterials in the Food Sector and Their Safety Assessment (Abstract book). Istituto Sup. di Sanità, Rome, p. 38.

Carbone, K., Garrigós, M.C., Jiménez, A., 2016. Polyphenols: from wastes to high added value by-products. In: Atta-ur-Rhaman (Ed.), Frontiers in Natural Product Chemistry. Publishing Bentham Science, Cambridge, pp. 115–178.

Cecchini, F., Moretti, S., Giannini, B., Carbone, K., 2013. Phytochemical profiles and antiradical capacity of grape seed extracts from different Italian cultivars: reusing of winery by-products. In: Carbone, Katya (Ed.), Cultivars: Chemical Properties, Antioxidant Activities and Health Benefits. Publishing Nova Science, New York, pp. 137–156.

Cruz, D., Falé, P.L., Mourato, A., Vaz, P.D., Serralheiro, M.L., Lino, A.R.L., 2010. Preparation and physicochemical characterization of Ag nanoparticles biosynthesized by Lippia citriodora (Lemon Verbena). Colloids Surf. B: Biointerfaces 81, 67–73.

Duan, S., Ai, Y.J., Hu, W., Luo, Y., 2014. Roles of plasmonic excitation and protonation on photoreactions of p-aminobenzenethiol on Ag nanoparticles. J. Phys. Chem. C 118, 6893–6902.

Ealia, S.A.M., Saravanakumar, M.P., 2017. A review on the classification, characterisation, synthesis of nanoparticles and their application. In: IOP Conference Series: Materials Science and Engineering, vol. 263, No. 3. IOP Publishing, p. 032019.

El-Ansary, A., Faddah, L.M., 2010. Nanoparticles as biochemical sensors. Nanotechnology Sci. Appl. 3, 65.

Gallo, V., Mastrorilli, P., Cafagna, I., Nitti, G.I., Latronico, M., Longobardi, F., Schütz, B., 2014. Effects of agronomical practices on chemical composition of table grapes evaluated by NMR spectroscopy. J. Food Compos. Anal. 35, 44–52.

Gan, P.P., Ng, S.H., Huang, Y., Li, S.F.Y., 2012. Green synthesis of gold nanoparticles using palm oil mill effluent (POME): a low-cost and eco-friendly viable approach. Bioresour. Technol. 113, 132–135.

Giovanni, M., Pumera, M., 2012. Size dependant electrochemical behavior of silver nanoparticles with sizes of 10, 20, 40, 80 and 107 nm. Electroanalysis 24, 615–617.

Gnanajobitha, G., Paulkumar, K., Vanaja, M., Rajeshkumar, S., Malarkodi, C., Annadurai, G., Kannan, C., 2013. Fruit-mediated synthesis of silver nanoparticles using Vitis vinifera and evaluation of their antimicrobial efficacy. J. Nanostruct. Chem. 3, 67.

Gupta, H., Kumar, R., Park, H.S., Jeon, B.H., 2017. Photocatalytic efficiency of iron oxide nanoparticles for the degradation of priority pollutant anthracene. Geosyst. Eng. 20 (1), 21–27.

He, L., Lin, M., Li, H., Kim, N.J., 2010. Surface-enhanced Raman spectroscopy coupled with dendritic silver nanosubstrate for detection of restricted antibiotics. J. Raman Spectrosc. 41 (7), 739–744.

Huang, D., Ou, B., Prior, R.L., 2005. The chemistry behind antioxidant capacity assays. J. Agr. Food Chem. 53, 1841–1856.

Huang, L., Weng, X., Chen, Z., Megharaj, M., Naidu, R., 2014. Green synthesis of iron nanoparticles by various tea extracts: comparative study of the reactivity. Spectrochim. Acta A: Mol. Biomol. Spectrosc. 130, 295–301.

Ivanova, O.S., Zamborini, F.P., 2010. Size-dependent electrochemical oxidation of silver nanoparticles. J. Am. Chem. Soc. 132, 70–72.

Jo, Y.K., Kim, B.H., Jung, G., 2009. Antifungal activity of silver ions and nanoparticles on phytopathogenic fungi. Plant Dis. 93, 1037–1043.

Khadri, H., Alzohairy, M., Janardhan, A., Kumar, A.P., Narasimha, G., 2013. Green synthesis of silver nanoparticles with high fungicidal activity from olive seed extract. Adv. Nanopart. 2, 241.

Khalil, M.M., Ismail, E.H., El-Baghdady, K.Z., Mohamed, D., 2014. Green synthesis of silver nanoparticles using olive leaf extract and its antibacterial activity. Arab. J. Chem. 7, 1131–1139.

Khanday, W.A., Marrakchi, F., Asif, M., Hameed, B.H., 2017a. Mesoporous zeolite–activated carbon composite from oil palm ash as an effective adsorbent for methylene blue. J. Taiwan Inst. Chem. Eng. 70, 32–41.

Khanday, W.A., Asif, M., Hameed, B.H., 2017b. Cross-linked beads of activated oil palm ash zeolite/chitosan composite as a bio-adsorbent for the removal of methylene blue and acid blue 29 dyes. Int. J. Biol. Macromol. 95, 895–902.

Khanday, W.A., Hameed, B.H., 2018. Zeolite-hydroxyapatite-activated oil palm ash composite for antibiotic tetracycline adsorption. Fuel 215, 499–505.

Kim, J.S., Kuk, E., Yu, K.N., Kim, J.H., Park, S.J., Lee, H.J., Kim, Y. K., 2007. Antimicrobial effects of silver nanoparticles. Nanomedicine: Nanotechnol Biol. Med. 3, 95–101.

Kim, S.W., Jung, J.H., Lamsal, K., Kim, Y.S., Min, J.S., Lee, Y.S., 2012. Antifungal effects of silver nanoparticles (AgNPs) against various plant pathogenic fungi. Mycobiology 40, 53–58.

Kuppusamy, P., Yusoff, M.M., Maniam, G.P., Govindan, N., 2016. Biosynthesis of metallic nanoparticles using plant derivatives and their new avenues in pharmacological applications–an updated report. Saudi Pharm. J. 24, 473–484.

Leopoldini, M., Russo, N., Toscano, M., 2011. The molecular basis of working mechanism of natural polyphenolic antioxidants. Food Chem. 125, 288–306.

Li, P., Li, J., Wu, C., Wu, Q., Li, J., 2005. Synergistic antibacterial effects of β-lactam antibiotic combined with silver nanoparticles. Nanotechnology 16, 1912–1917.

Lin, D., Xing, B., 2007. Phytotoxicity of nanoparticles: inhibition of seed germination and root growth. Environ. Pollut. 150, 243–250.

Logaranjan, K., Devi, S., Pandian, K., 2012. Biogenic synthesis of silver nanoparticles using fruit extract of ficus carica and study its antimicrobial activity. Nano Biomed. Eng. 4, 177–182.

Logeswari, P., Silambarasan, S., Abraham, J., 2013. Ecofriendly synthesis of silver nanoparticles from commercially available plant powders and their antibacterial properties. Sci. Iran. 20, 1049–1054.

López-Rituerto, E., Savorani, F., Avenoza, A., Busto, J.H., Peregrina, J.M., Engelsen, S.B., 2012. Investigations of La Rioja terroir for wine production using 1H NMR metabolomics. J. Agr. Food Chem. 60, 3452–3461.

Makarov, V.V., Love, A.J., Sinitsyna, O.V., Makarova, S.S., Yaminsky, I.V., Taliansky, M.E., Kalinina, N.O., 2014. "Green" nanotechnologies: synthesis of metal nanoparticles using plants. Acta Naturae 6 (1 (20)).

Makris, D.P., Boskou, G., Andrikopoulos, N.K., 2007. Polyphenolic content and in vitro antioxidant characteristics of wine industry and other agri-food solid waste extracts. J. Food Compost. Anal. 20, 125–132.

Malešev, D., Kuntić, V., 2007. Investigation of metal-flavonoid chelates and the determination of flavonoids via metal-flavonoid complexing reactions. J. Serb. Chem. Soc. 72 (10), 921–939.

Mandke, M.V., Han, S.H., Pathan, H.M., 2012. Growth of silver dendritic nanostructures via electrochemical route. Cryst. Eng. Comm. 14, 86–89.

Mittal, A.K., Chisti, Y., Banerjee, U.C., 2013. Synthesis of metallic nanoparticles using plant extracts. Biotechnol. Adv. 31, 346–356.

MubarakAli, D., Thajuddin, N., Jeganathan, K., Gunasekaran, M., 2011. Plant extract mediated synthesis of silver and gold nanoparticles and its antibacterial activity against clinically isolated pathogens. Colloids Surf. B 85, 360–365.

Nidzworski, D., Pranszke, P., Grudniewska, M., Król, E., Gromadzka, B., 2014. Universal biosensor for detection of influenza virus. Biosens. Bioelectron. 59, 239–242.

Picone, G., Mezzetti, B., Babini, E., Capocasa, F., Placucci, G., Capozzi, F., 2011. Unsupervised principal component analysis of NMR metabolic profiles for the assessment of substantial equivalence of transgenic grapes (Vitis vinifera). J. Agr. Food Chem. 59, 9271–9279.

Rajan, R., Chandran, K., Harper, S.L., Yun, S.I., Kalaichelvan, P.T., 2015. Plant extract synthesized silver nanoparticles: an ongoing source of novel biocompatible materials. Ind. Crop. Prod. 70, 356–373.

Saratale, R.G., Karuppusamy, I., Saratale, G.D., Pugazhendhi, A., Kumar, G., Park, Y., Shin, H.S., 2018. A comprehensive review on green nanomaterials using biological systems: recent perception and their future applications. Colloid Surf. B 170, 20–35.

Song, J.Y., Jang, H.K., Kim, B.S., 2009. Biological synthesis of gold nanoparticles using Magnolia kobus and Diopyros kaki leaf extracts. Process Biochem. 44, 1133–1138.

Tang, S., Meng, X., Lu, H., Zhu, S., 2009. PVP-assisted sonoelectrochemical growth of silver nanostructures with various shapes. Mater. Chem. Phys. 116, 464–468.

Terenteva, E.A., Apyari, V.V., Dmitrienko, S.G., Zolotov, Y.A., 2015. Formation of plasmonic silver nanoparticles by flavonoid reduction: A comparative study and application for determination of these substances. Spectrochim. Acta A Mol. Biomol. Spectrosc. 151, 89–95.

Thombre, R., Parekh, F., Lekshminarayanan, P., Francis, G., 2012. Studies on antibacterial and antifungal activity of silver nanoparticles synthesized using Artocarpus heterophyllus leaf extract. Biotechnol. Bioinform. Bioeng 2, 632-.

Vitiello, G., Silvestri, B., Luciani, G., 2018. Learning from nature: bioinspired strategies towards antimicrobial nanostructured systems. Curr. Top. Med. Chem. 18 (1), 22–41.

Welch, C.M., Compton, R.G., 2006. The use of nanoparticles in electroanalysis: a review. Anal. Bioanal. Chem. 38, 601–619.

Wen, X., Xie, Y.T., Mak, W.C., Cheung, K.Y., Li, X.Y., Renneberg, R., Yang, S., 2006. Dendritic nanostructures of silver: facile synthesis, structural characterizations, and sensing applications. Langmuir 22, 4836–4842.